




Primary fibroblast co-culture stimulates growth and metabolism in *Sdhb*-impaired mouse pheochromocytoma MTT cells

Susan Richter¹ · Vanessa D'Antongiovanni² · Serena Martinelli² · Nicole Bechmann¹ · Maria Riverso² · David M. Poitz¹ · Karel Pacak³ · Graeme Eisenhofer¹ · Massimo Mannelli² · Elena Rapizzi⁴ 

Received: 24 April 2018 / Accepted: 7 August 2018
© Springer-Verlag GmbH Germany, part of Springer Nature 2018

Abstract

Pheochromocytomas and paragangliomas (PGLs) due to mutations of succinate dehydrogenase (SDH) B, a subunit of the SDH complex with a role in the Krebs cycle and the respiratory chain, tend to be larger at diagnosis and more prone to metastatic disease than other tumors. This presentation contrasts with the behavior of some cell line models of *SDHB* impairment, which show reduced growth compared to wild type. We hypothesize that reduced growth of *SDHB*-impaired monolayer culture models might reflect lack of support from sources within the tumor microenvironment. The present study therefore investigates how the microenvironment, modeled here by fibroblast co-culture, modulates cell metabolism, growth and invasion in an *Sdhb*-impaired mouse pheochromocytoma cell line. We employed two different constructs of short hairpin RNA to knockdown *Sdhb* and compared growth in a monolayer with and without fibroblast co-culture. *Sdhb*-silenced cells showed functional impairment of SDH with elevated succinate to fumarate ratio and decreased oxidative capacity. Cell growth was delayed with an increase in doubling time of 2 h or 20 h. Clonogenic cell survival and viability, on the other hand, were either unchanged or increased compared to control. In standard monolayer culture, no differences in pro-metastatic features were present. Co-culture with primary mouse fibroblast reversed the difference of proliferation between control and *Sdhb* knockdown but was unable to significantly influence invasiveness under these culture conditions. Metabolic studies identified that lactate secreted by fibroblasts was taken up preferentially by *Sdhb*-silenced cells. In summary, the present study identified a potential role for the tumor microenvironment in influencing phenotypic features of *SDHB*-mutated PGLs, providing a basis for the use of therapies targeted towards the tumor microenvironment.

Keywords Pheochromocytoma · Paraganglioma · Tumor microenvironment · Succinate dehydrogenase · Lactate

Susan Richter and Vanessa D'Antongiovanni contributed equally to this work.

✉ Elena Rapizzi
elena.rapizzi@unifi.it

- ¹ University Hospital Carl Gustav Carus, Institute of Clinical Chemistry and Laboratory Medicine, Technische Universität Dresden, Dresden, Germany
- ² Department of Experimental and Clinical Biomedical Sciences, University of Florence, Florence, Italy
- ³ Eunice Kennedy Shriver National Institute of Child Health and Human Development, National Institutes of Health, Bethesda, USA
- ⁴ Department of Experimental and Clinical Medicine, University of Florence, Viale, Pieraccini 6, 50139 Florence, Italy

Introduction

Pheochromocytomas (PHEOs) and paragangliomas (PGLs) are neural crest-derived tumors originating from cells of the adrenal medulla or associated with the autonomic nervous system. About 40% of tumors are genetically inherited involving germline mutations in at least 15 currently known susceptibility genes (Favier et al. 2015). These include genes encoding the four subunits of the mitochondrial enzyme succinate dehydrogenase (SDH), which functions in mitochondrial electron transport as complex II and in tricarboxylic acid (TCA) cycle by catalyzing the oxidation of succinate to fumarate. Impairment of SDH activity causes accumulation of the oncometabolite, succinate, affecting a wide spectrum of pathways ranging from pseudo-hypoxia signaling to

epigenetic reprogramming (Jochmanova and Pacak 2016; Mannelli et al. 2015).

SDHB-mutated PHEOs/PGLs are larger when diagnosed, less differentiated and contain lower amounts of catecholamines compared to other PHEOs/PGLs (Eisenhofer et al. 2012). Most importantly, the tumors are more prone to malignant progression compared to other PHEOs/PGLs (Gimenez-Roqueplo et al. 2003). Patients with *SDHB*-mutated PHEOs/PGLs present, at a relatively young age and often in childhood, when there is particularly a high risk of, metastatic disease (King et al. 2011; Pamporaki et al. 2017). Although large tumor size in patients with *SDHB* mutations could simply reflect a delay in diagnosis, the large size and associated propensity of these tumors to metastasize have also been suggested to reflect diversion of energy from maintaining a differentiated secretory phenotype to enhancement of uncontrolled cellular division (Eisenhofer et al. 2012). As further discussed, it is also possible that other cells of the tumor microenvironment contribute to tumor cell proliferation.

Cell line models of *SDHB* impairment showed differential effects on growth depending on the parent cell line. *SDHB*-impaired hepatocellular carcinoma Hep3B, and kidney mouse cells exhibit reduced growth whereas accelerated proliferation has been described after *SDHB* knockdown or knockout in the osteosarcoma cell line 143B, mouse ovarian cancer cells and the human neuroblastoma cell line SK-N-AS (Aspuria et al. 2014; Cardaci et al. 2015; Cervera et al. 2008; Guzy et al. 2008). In mouse chromaffin progenitor cells, representing a more relevant model for PHEO/PGL but lacking the production of catecholamines, proliferation of *Sdhb* knockout cell clones was also reduced (Letouze et al. 2013).

Solid tumors are very complex tissues containing not only cancer cells but also extracellular matrix and non-transformed stromal cells, including endothelial cells, fibroblasts and immune cells, altogether referred to as the tumor microenvironment. Over the past decade, it has become evident that the continual interplay between cancer and stromal cells generates a positive loop aiding cancer cells in surviving and proliferating in hostile environments (Chiarugi and Cirri 2016; Hanahan and Coussens 2012; Quail and Joyce 2013). We therefore hypothesize that the tumor microenvironment is a driving force in stimulating growth in *SDHB*-impaired cells, thereby explaining the discrepancy between the clinical presentation of *SDHB*-mutated PHEO/PGL and chromaffin cell culture model systems. To address this hypothesis, we investigate the impact of the microenvironment, represented by primary mouse fibroblasts in a co-culture model, on monolayer growth; pro-metastatic features; and metabolism of the mouse pheochromocytoma cell line, MTT, with and without knockdown of *Sdhb*.

Materials and methods

Cell culture

Mouse PHEO-derived MTT cells were cultivated in Dulbecco's modified Eagle's medium (DMEM) plus GlutaMAX supplemented with 10% horse serum (HS) and 5% fetal calf serum (FCS) on collagen A-coated plasticware (Martiniova et al. 2009). For the microenvironment studies, MTT cells were cultivated in DMEM plus 2 mM glutamine, 10% FCS and 5% HS. The transduced cells were cultivated under the addition of puromycin (1 µg/ml) treatment. In all cases, cells were cultured at 37 °C, 5% CO₂ and 95% humidity and tested to be mycoplasma free (Venor[®]GeM Classic, Minerva Biolabs). For all experiments, cells were grown until 70–80% confluence, trypsinized (trypsin/EDTA; 0.05%/0.02%) and if not indicated otherwise, seeded in antibiotic-free complete medium.

Primary fibroblasts were obtained from legs of newborn mice by enzymatic digestion with trypsin. The cell suspension was plated for 1 h at 37 °C after which adherent cells, mostly fibroblasts, were washed twice with phosphate-buffered saline (PBS) and were grown in DMEM + 10% FCS. Co-cultures were performed in multiwell plates with inserts separating tumor cells from fibroblasts by permeable membranes (0.4-µm pores; Greiner Bio-One International, Germany) in serum-free DMEM with 0.1% bovine serum albumin (BSA).

Intracellular adenosine triphosphate (ATP) and lactate values and glucose and lactate uptake measurements were normalized to the cell number. To this end, cells were seeded in replicates in extra wells, exclusively for cell counting, for each experimental condition. At the end of each experiment, cell number was assessed by a hemocytometer after trypsin treatment.

Sdhb silencing

Sdhb was stably knocked down by viral transduction with MISSION[™] lentiviral particles (Sigma-Aldrich) containing two different constructs of short hairpin RNA (shRNA) against murine *Sdhb* (63; 64; Clone ID TRCN0000041763 and TRCN0000041764) or a non-targeting shRNA construct as control (SHC002V). Cultures were treated with 1 µg/ml puromycin to select for viral DNA integration.

Cell counting and proliferation

Cells were seeded at 10⁵/ml with a volume of 2 ml into six-well plates. Cell number was assessed after trypsin treatment by a hemocytometer after 48 h, 72 h and 144 h. Single cells of each clump were counted. Doubling times were calculated using the least square fitting method of a time series (Roth

V. 2006 Doubling Time Computing, available from: <http://www.doubling-time.com/compute.php>.

For co-culture experiments, MTT cells were seeded (7.5×10^4) into 12-well plate inserts (control single culture) and for co-culture, primary fibroblasts were seeded (1.5×10^5) in the well below. Cells were serum starved for 24 h before starting the co-culture in serum-free medium and cells were counted after 24 h, 48 h, and 72 h.

Thymidine incorporation was measured by adding [^3H]thymidine (0.5 $\mu\text{Ci}/\text{well}$) for the last 2 h of incubation to both co-cultured and single-cultured MTT. Cells were washed twice in ice-cold PBS before the addition of 500 μl of 10% trichloroacetic acid (TCA) for 30 min at 4 °C and then washed twice with 250 μl of 5% TCA. Cells were lysed in 0.25 M NaOH (500 $\mu\text{l}/\text{well}$) for 1 h at 37 °C. Incorporation of [^3H]thymidine was measured by scintillation counting (Tri-Carb2800 TR Liquid Scintillation Analyzer, PerkinElmer).

Apoptosis assay

Induction of apoptosis was evaluated using Caspase-Glo 3/7 assay (Promega, Madison, WI). Cells were plated at 5×10^4 /well in a 96-well plate. After 24 h, the wells were washed twice in PBS and the medium was replaced with 100 μl of fresh medium (control) or cancer-activated fibroblast (CAF)-conditioned medium. After 24 h of treatment, 100 μl of Caspase-Glo 3/7 reagents were added. The plates were read after 40 min using the Victor³ 1420 Multilabel Counter (Packard Instruments, PerkinElmer).

Cell viability

Cells were seeded in 96-well plates at 3.5×10^4 /well and incubated for 24 h. The viability assay was performed according to the manufacturer's instructions. Briefly, 20 μl of CellTiter 96[®] AQueous One Solution (Promega) was added to each well. After 3 h of incubation, absorption was measured at 492 nm using the Victor³ 1420 Multilabel Counter (Packard Instruments, PerkinElmer).

Clonogenic cell survival assay

To determine differences in clonogenic cell survival, an optimized cell number (1000 cells) was plated in six-well plates. After a growing period of 11 days, cells were washed with PBS and fixed in methanol/PBS (1:1; v/v) for 5 min followed by methanol for 10 min. Cells were stained with a 1% aqueous crystal violet solution for 15 min under agitation. After removal of the staining solution, plates were washed with water and air-dried. Colonies larger than 50 cells were counted under a microscope (Carl Zeiss Telaval 3).

Catecholamines

Cells were extracted with 0.4 M perchloric acid containing 0.5 mM EDTA in Milli-Q water. Lysates were cleared by centrifugation and catecholamines were measured by HPLC as described previously (Eisenhofer et al. 1986).

Mass spectrometric measurements of Krebs cycle metabolites and amino acids

Metabolites were extracted from cell cultures after four washes with PBS using ice-cold methanol. After centrifugation, extracts were dried down using a SpeedVac concentrator (Thermo Scientific). Metabolites were resuspended in mobile phase and quantified by ultra high-pressure liquid chromatography tandem mass spectrometry (LC-MS/MS) as described previously (Richter et al. 2014). Values were normalized to cell number.

Oxygen consumption/extracellular acidification

Cells were seeded at 4×10^4 /well in a 96-well plate suitable for use with the Seahorse XF96 Analyzer (Agilent Technologies). The Mito Stress Test assay was carried out according to the manufacturer's recommendations and oxygen consumption and extracellular acidification were measured. Cell normalization was carried out in the assay plates by CyQUANT[®] Cell Proliferation Assay (Thermo Fisher).

Quantitative real-time PCR

Total RNA was extracted from homogenized tissues using the RNeasy[®] Micro Kit (Qiagen) and cDNA was generated using the GeneAmp[®] RNA PCR Kit (Applied Biosystems). Real-time quantitative PCR (qPCR) was performed on a CFX Connect Real-Time PCR Detection System (Bio-Rad) with the Rotor-Gene SYBR Green qRT-PCR reagent (Qiagen). The following primers were employed: β -actin forward 5'-AAGGCCAACCGTGAAAAGAT-3' and reverse 5'-GTGGTACGACCAGAGGCATAC-3'; Sdhb forward 5'-AGCTACTGGTGGAAACGGAGA-3' and reverse 5'-GCAGCGGTAGACAGAGAAGG-3'; tyrosine hydroxylase (TH) forward 5'-GGTATACGCCACGCTGAAGG-3' and reverse 5'-TAGCCACAGTACCGTTCCAGA-3'; DOPA decarboxylase (DDC) forward 5'-CCTGATTCCATTCTTTGTGG-3' and reverse 5'-ATCTGCAAACCTCCACACCAT-3'; and dopamine β -hydroxylase (DBH) forward 5'-ACAGGTTTACAGCAGTGAGGAG-3' and reverse 5'-CGGACAGCAGAAGTCTTGTT-3'. DNA amplification and subsequent melting curve analysis were performed with the following program conditions: 95 °C for 2 min, 40 cycles of 95 °C for 5 s and 60 °C for 30 s, 95 °C for 10 s and 55–95 °C in 0.5 °C increments.

Western blot

Cells were lysed in CellLytic M buffer (Sigma-Aldrich) or as described by Rapizzi et al. (Rapizzi et al. 2015) and protein was quantified with the Bradford assay. Proteins were separated on 4–20% sodium dodecyl sulfate polyacrylamide gels (C.B.S. Scientific) and transferred to PVDF membranes (Fisher Scientific or Immobilon, Millipore, MA, USA). Primary antibodies against actin (MAB1510R, Millipore, or sc-1615, Santa Cruz), SDHB (ab14714, Abcam), TH (NB300-109, Novus Biologicals), phospho S40-TH (ab51206, Abcam) and MCT4 (sc-50329, Santa Cruz) were used. Secondary antibodies were obtained from Santa Cruz (anti-mouse sc-2005, anti-rabbit sc-2004, anti-goat sc-2020). Membranes were blocked with 5% fat-free milk diluted in PBS with 0.1% Tween 20. Protein bands were detected with ECL reagents (femtoLUCENT peroxide solution, G-Biosciences, or Immobilon, Millipore). Densitometry was undertaken using ImageJ software.

Intracellular ATP

ATP levels were measured using CellTiter-Glo luminescent cell viability assay (Promega). This assay was performed according to the manufacturer's protocol. Briefly, tumor cells were seeded into 12-well plates in single culture or in co-culture with mouse primary fibroblasts in a 1:2 ratio (7.5×10^4 and 1.5×10^5 , respectively). After 16 h, cells were washed twice in PBS and then cells were left to grow for 48 h in serum-free DMEM. Cells were incubated with 125 μ l of CellTiter-Glo reagent. The cultures were shaken at 300 rpm for 5 min and then incubated at room temperature for 25 min to stabilize the luminescent signal. Luminescence was measured using the Victor³ 1420 Multilabel Counter (Packard Instruments, PerkinElmer) and normalized to a number of cells.

Glucose and lactate uptake

To determine glucose and lactate uptake, tumor cells were seeded in six-well plates (1.5×10^5), in single culture or in co-culture with fibroblasts (3×10^5). After 16 h, cells were washed twice in PBS and left to grow for 48 h in serum-free DMEM. 2-Deoxy-glucose or lactate uptake was evaluated in a buffered solution (140 mM NaCl, 20 mM HEPES/Na, 2.5 mM MgSO₄, 1 mM CaCl₂, and 5 mM KCl, pH 7.4) containing 0.5 μ Ci/ml [³H]deoxyglucose or 1 μ Ci/ml [U-¹⁴C]lactate. The reaction was maintained at 37 °C for 15 min. Cells were subsequently washed with cold PBS and lysed with 0.1 M NaOH. Incorporated radioactivity was assayed by liquid scintillation counting (Rapizzi et al. 2014). Values were normalized to cell number.

Lactate measurement

Lactate was measured using the Lactate Colorimetric/Fluorometric Assay Kit (BioVision, Milpitas, CA, USA) according to the manufacturer's protocol. Briefly, tumor cells were seeded into 12-well plates (7.5×10^4) in single culture or in co-culture with mouse primary fibroblasts (1.5×10^5). They were left to grow for 48 h in serum-free DMEM. For intracellular lactate assay, samples were diluted 1:2 with buffer provided in the kit to 50 μ l total volume and then mixed with 50 μ l of mix solution provided in the kit in a 96-well plate. The plate was then incubated at 37 °C for 30 min. The absorbance was measured at 570 nm. For extracellular lactate assay, the inserts of the co-cultures were separated from fibroblasts. The inserts were put into new empty plates and the medium was replaced with a fresh one. Medium was replaced with a fresh one also in fibroblasts and the separated cultures were left for 24 h. Medium samples were then diluted 1:5 and processed as described above. The luminescence signal was revealed using the Victor³ 1420 Multilabel Counter (Packard Instruments, PerkinElmer) and normalized on a number of cells.

Assessment of pro-metastatic features in single culture

Adhesion assay

Cells (4×10^5) were plated in each well of a six-well plate (pre-culture). Twenty-four-well plates were coated with collagen A. After 24 h, the collagen-coated plates were washed twice with PBS and unspecific binding sites were blocked with PBS containing 2% BSA for 1 h at 37 °C. Cells were washed twice with PBS, detached with trypsin (comment: detachment with EDTA or Accutase was not successful for the cells) and resuspended in DMEM + GlutaMAX containing 0.2% BSA. Cells (2×10^5 /well) were seeded in the collagen- or fibronectin-coated wells and allowed to adhere for 30 min. Non-adherent cells were washed away with PBS. The remaining cells were fixed for 5 min in PBS/methanol followed by 10 min in 100% methanol and stained for 15 min with crystal violet. After four washing steps with tap water, cells were air-dried and lysed with PBS containing 0.5% Triton X-100 for 30 min under continuous shaking. After transfer in a 96-well plate, absorption at 550 nm was measured by Victor³ 1420 Multilabel Counter (PerkinElmer). 0.5% Triton X-100 in PBS was used as a blank.

Migration assay

The ability of MTT cells to migrate through 8- μ m pores was measured by using TC Inserts (Sarstedt; Item No. 83.3931.800). Cells (5×10^6) were plated in cell culture flasks

(T75). After 24 h, the medium was removed and DMEM + GlutaMAX containing 0.2% BSA was added, followed by 24 h of incubation. Cells were washed with PBS, trypsinized and diluted in DMEM containing 0.2% BSA up to a concentration of 1×10^6 /ml. As a chemoattractant, complete DMEM + GlutaMAX (10% HS, 5% FCS, 1 mM sodium pyruvate) was filled in each well of a 12-well plate and the single cell suspensions (2×10^5 cells/insert) were added in the upper compartment of the cell culture insert. After 24 h of incubation, culture medium was replaced by DMEM + GlutaMAX (0.2% BSA) containing 1 μ M calcein for 1 h at 37 °C (BD™ Calcein AM Fluorescent Dye, BD Biosciences). Afterwards, the lower compartment was washed with PBS and migrated cells were trypsinized. The fluorescence of calcein-stained cells was measured at 485Ex/528Em by Victor3 1420 Multilabel Counter (PerkinElmer).

Invasion assay

For invasion experiments, the TC Inserts were coated with the basement membrane Matrigel (Matrigel (BD Bioscience)/DMEM + GlutaMAX, 1:3, v/v) and the experimental procedure was performed as described for the migration assay.

Invasion assay with fibroblast co-culture

Matrigel solution (Corning® Matrigel® Basement Membrane Matrix BD Biosciences, concentration 9.7 mg/ml) was mixed 1:1 with DMEM to obtain the final solution of 0.3% Matrigel. The solution was added to the growth surface of culture inserts for multiwell plates (transparent membrane with 8- μ m pores) and left to be hydrated overnight at 37 °C. Cells (6×10^4 cells/well) were seeded on the Matrigel in the Transwell insert and placed in the multiwell plates with fibroblasts. As controls, we used cells in single culture (without fibroblasts in the bottom well plate). After 72 h, the cells were fixed in methanol for 10 min and stained with crystal violet. Bright-field images were acquired by inverted microscopy (Axiovert25 with AxioCam MRe digital camera, Zeiss). For quantification, crystal violet was dissolved in 10% acetic acid and absorbance was measured at a wavelength of 595 nm.

Zymography

Confluent cells were washed twice in PBS and serum starved in DMEM containing 0.1% BSA. Tumor cells were treated with CAF-conditioned medium or non-conditioned medium for 72 h. Thereafter, media were replaced with fresh DMEM containing 0.1% BSA and harvested for zymography assay after 48 h. Cells were counted for normalization.

Supernatants were centrifuged for 10 min at 10,000g at 4 °C. To each, samples (45 μ l) were added 5 μ l of sample buffer (4% SDS, 100 mM Tris HCl at pH 6.8, 20% glycerol,

and 0.01% blue bromophenol) without beta-mercaptoethanol. Samples were separated in an 8% acrylamide gel containing 0.1% gelatin. Gels were washed twice for 30 min with 2% Triton X-100, then for 30 min in the reaction buffer (50 mM Tris HCl at pH 7.5, 200 mM NaCl, 5 mM CaCl₂) and finally, incubated overnight at 37 °C in reaction buffer. Gels were stained with Coomassie Brilliant Blue R-250 (Amersham Pharmacia). As a result, visible light bands relating to enzymatic digestion of gelatin by metalloprotease became evident. Densitometry was undertaken using Image Lab software.

Statistical analysis

Statistical analysis was performed using SigmaPlot 12.5 and JMP Pro 12. Comparisons between multiple groups were undertaken by least square multivariate analysis with the Tukey-Kramer post hoc test, or one-way ANOVA with the Bonferroni post hoc test or Dunnett's post hoc test; two groups were compared by the Wilcoxon rank-sum test. Values are provided as mean \pm SEM.

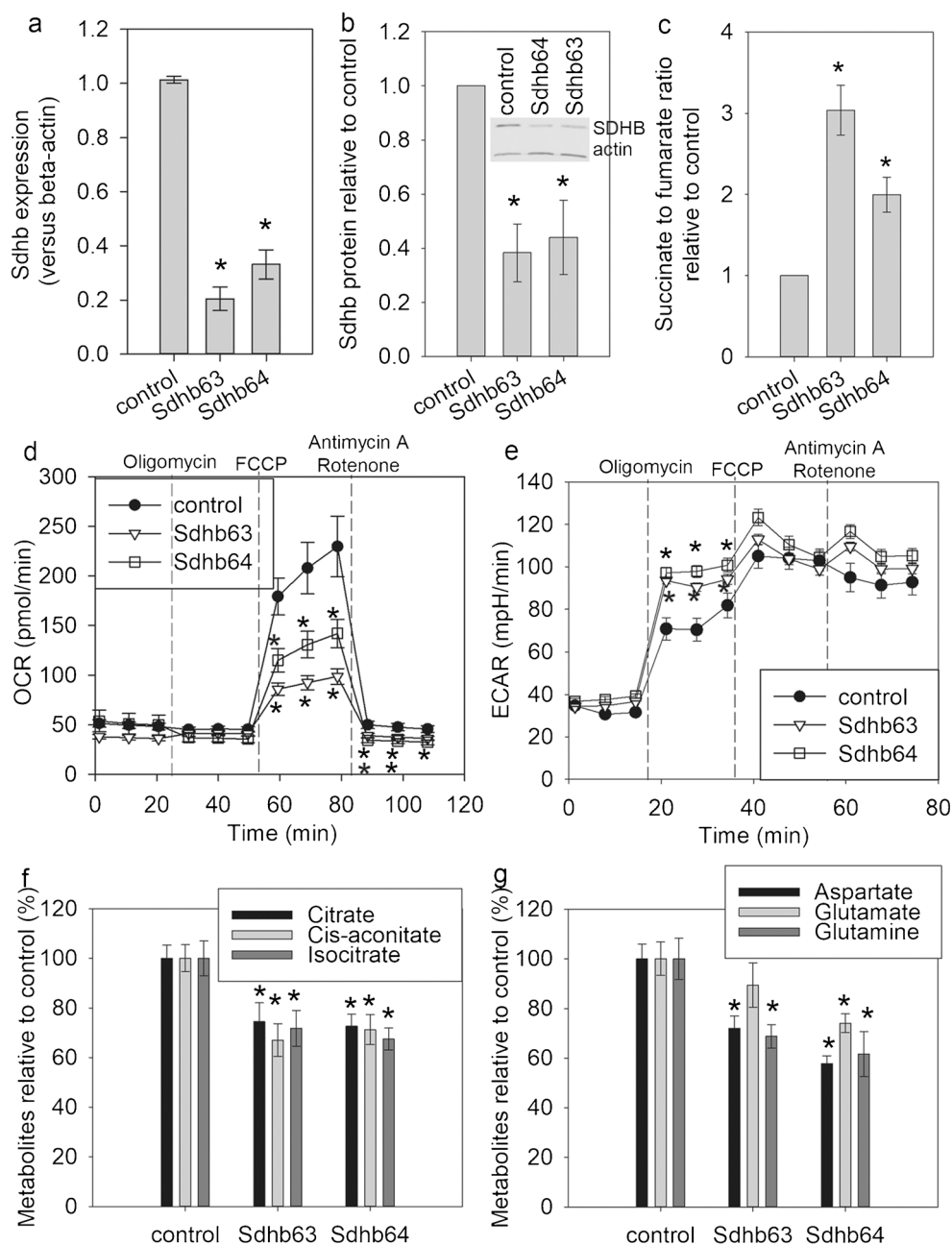
Results

Characterization of MTT cells with *Sdhb* silencing in monolayer culture

Transduction with lentiviruses encoding shRNAs (63 and 64) against the murine gene achieved a decrease of *Sdhb* mRNA by 79% with shRNA-63 and 67% with shRNA-64, translating to a protein reduction of 62% and 56%, respectively (Fig. 1a, b). Functional impairment was confirmed by elevated succinate to fumarate ratios of threefold for shRNA-63 and twofold for shRNA-64 and reduced maximal respiratory capacity measured with the addition of the mitochondrial oxidative phosphorylation uncoupler carbonyl cyanide-4-(trifluoromethoxy)phenylhydrazone (FCCP) (Fig. 1c, d). Additionally, *Sdhb*-silenced cells showed reduced respiration when the electron transport chain was inhibited completely by antimycin A and rotenone. An impacted respiratory phenotype was, however, only observed with high nutritional concentrations of 25 mM glucose, 4 mM glutamine and 1 mM pyruvate. Reduction to 10 mM glucose, 2 mM glutamine and 1 mM pyruvate abolished the effect on respiration (data not shown). Extracellular acidification was unchanged between *Sdhb* knockdown and control with high concentrations of nutrients, whereas ATP synthase inhibition with oligomycin led to a significant increase in glycolytic capacity for *Sdhb*-silenced cells when less nutrients were available (Fig. 1e).

In agreement with patient tumors, Krebs cycle metabolites citrate, *cis*-aconitate and isocitrate, as well as amino acids aspartate, glutamate and glutamine are significantly reduced

Fig. 1 Confirmation of *Sdhb* knockdown in MTT on mRNA (a), protein level (b) and function (c–e). **a** Real-time qPCR results of three biological replicates. **b** Densitometry of four different protein lysates for each sample type analyzed on four different western blots with one representative western blot displayed. **c** Succinate-to-fumarate ratio measured by LC-MS/MS, three experiments with three biological replicates each. **d** Oxygen consumption rate (OCR) in 25 mM glucose, 4 mM glutamine and 1 mM pyruvate measured by the Seahorse XF Analyzer shows decreased maximal respiratory capacity with the uncoupler FCCP, six biological replicates. **e** Extracellular acidification rate (ECAR) in 10 mM glucose, 2 mM glutamine and 1 mM pyruvate measured by the Seahorse XF Analyzer shows increased maximal glycolytic capacity with oligomycin, eight biological replicates. **f, g** Krebs cycle metabolites and amino acids measured by LC-MS/MS in three experiments with three replicates. Asterisks indicate significance ($*p < 0.05$, $**p < 0.001$) by one-way ANOVA with the Bonferroni post hoc test compared to control



in *Sdhb*-silenced MTT cells compared to control, further indicating functional impairment of SDH (Imperiale et al. 2013; Lussey-Lepoutre et al. 2015; Richter et al. 2014) (Fig. 1f, g).

Population doubling time in the monolayer was reduced in MTT *Sdhb* knockdown cell lines compared to control with 35 h for control and 55 h and 37 h for shRNA-63 and shRNA-64, respectively, under conditions of serum and high nutrient availability (Fig. 2a). *Sdhb* knockdown cell lines showed a more three-dimensional growth with a stronger clumping behavior (Fig. 2b', b'') compared to control (Fig. 2b). Interestingly, cell viability measured as the capacity to reduce tetrazolium salts was higher in MTT cells with *Sdhb* knockdown, whereas cell survival by colony formation assay

was similar to control with a non-significant increase for shRNA-63 (Fig. 2c, d, respectively).

Control and *Sdhb*-silenced cells showed similar pro-metastatic features (Fig. 2e–g). Interestingly, MTT cells have intrinsically a very low migratory capacity but move much better in the presence of Matrigel. For this reason, only invasion was quantified in later experiments.

To further characterize our cell model, the chromaffin phenotype of catecholamine production was evaluated. Knockdown of *Sdhb* increased cellular contents of dopamine by more than twofold in both cell lines, whereas norepinephrine was only significantly higher for shRNA-64, both with and without dexamethasone stimulation (Fig. 2h). The

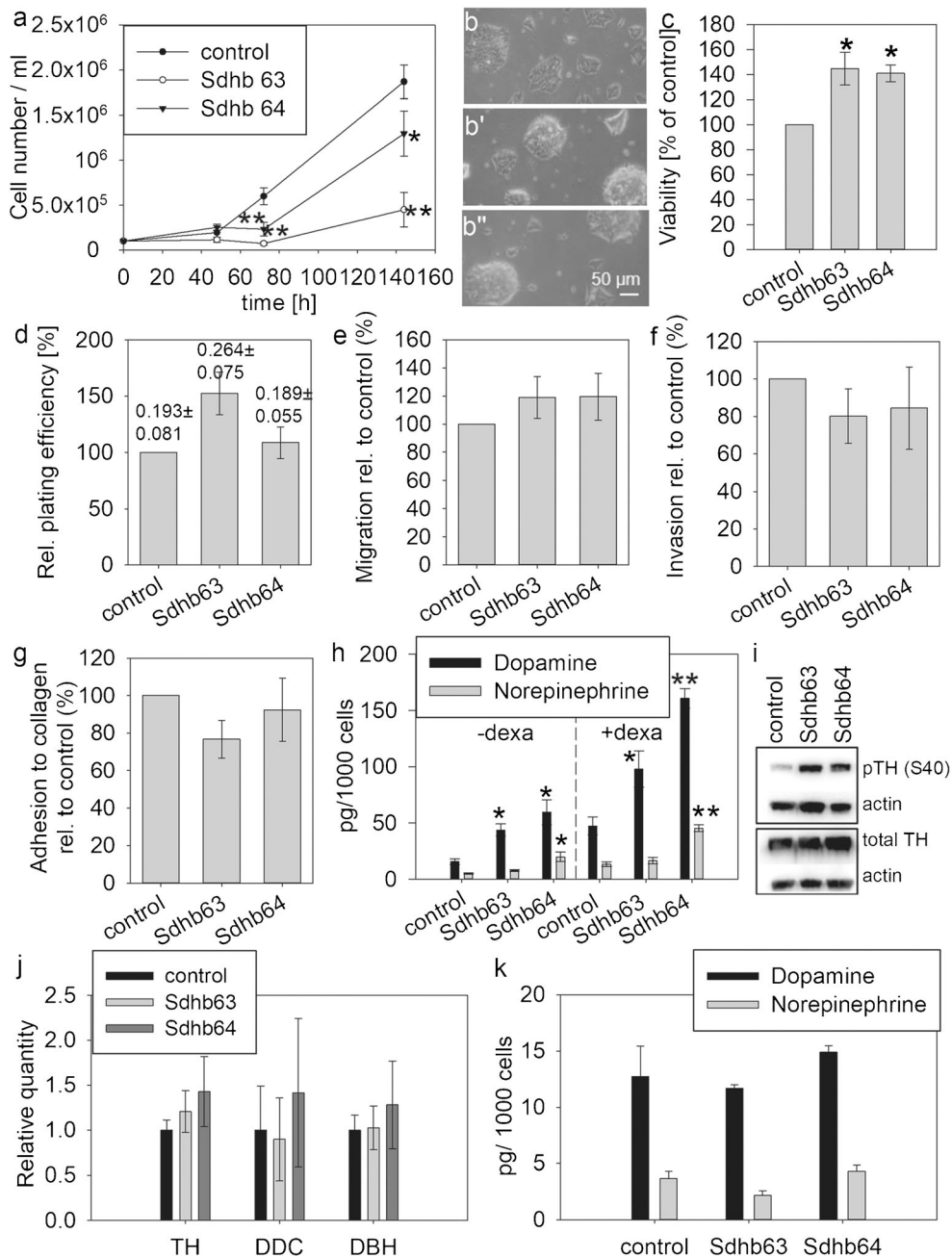


Fig. 2 Characterization of *Sdhb* knockdown MTT cells under standard monolayer culture conditions. **a** Cell number was measured in three independent experiments with two biological replicates each. Control (**b**), *Sdhb63* (**b'**), *Sdhb64* (**b''**). Pictures were recorded at $\times 10$ objective magnification using a light microscope. Asterisks indicate significance ($*p < 0.05$, $**p < 0.001$) compared to control by least square multivariate analysis with the Tukey-Kramer post hoc test. **c** Viability assessed by redutive capacity was measured in four experiments with 18 biological replicates each. **d** Colony formation assay, three experiments with three biological replicates. Numbers above the bars indicate absolute plate efficiencies. **e** Pro-metastatic features were characterized in MTT cells

grown in a monolayer in four or five experiments each. Migration was assessed by Transwell assay, $n = 4$. **f** Invasion was measured by Transwell assay with Matrigel coating, $n = 4$. **g** Adhesion to collagen, $n = 5$. **h** Intracellular catecholamines with (+ dexa) and without (- dexa) dexamethasone stimulation (3 days), three experiments with three biological replicates. **i** Gene expression of enzymes of the catecholamine synthesis pathway, $n = 3$. Expression was normalized against β -actin. **j** Western blot for total and phospho S40 tyrosine hydroxylase. **k** Intracellular catecholamine levels under serum-free culture with 0.1% BSA. Asterisks indicate significance ($*p < 0.05$, $**p < 0.001$) compared to control by one-way ANOVA with the Bonferroni post hoc test

dopamine increase was mediated by changes in phosphorylation of serine residue 40 of tyrosine hydroxylase (Fig. 2i) but not through altered expression of any of the enzymes

catalyzing catecholamine synthesis (Fig. 2j). To investigate whether catecholamine increases could be mediated through factors in the serum, we cultured our cells under serum-free

conditions, where we found similar levels of catecholamines in control and *Sdhb*-silenced cells (Fig. 2k).

Fibroblast co-culture influences the proliferative and metabolic phenotype of *Sdhb*-silenced MTT cells

The influence of fibroblast co-culture was evaluated in subsequent experiments in MTT cell line Sdhb63, which had a stronger *Sdhb* knockdown with higher succinate accumulation. All cultures were performed in serum-free medium, in order to assess fibroblast-mediated growth effects without the presence of undefined factors (Fig. 3a). *Sdhb*-silenced cells grew slower compared to control cells in serum-free culture, as was shown with serum. Fibroblasts were able to stimulate the growth of MTT control and *Sdhb* knockdown cells. A cell number increase after 72 h with co-culture was significantly greater in *Sdhb* knockdown compared to control cells, indicating a reversal of the growth delay found under serum conditions (Fig. 3b). These effects were followed up by two further methods. Thymidine incorporation was significantly increased by fibroblasts in both MTT cell lines but *Sdhb*-silenced cells showed an additional significant increase compared to control (Fig. 3c). Apoptosis was also increased through fibroblast co-culture but *Sdhb* knockdown cells had reduced levels of caspase activity under serum-free and fibroblast co-culture conditions (Fig. 3d). Co-culture also affected the morphology of MTT cells; control and *Sdhb*-silenced cells assumed an elongated form (Fig. 3e', e'') in contrast to a more rounded shape with a tendency to cell aggregation in single cell culture (Fig. 3e, e'').

Although fibroblasts had a significant effect on cell proliferation in monolayer culture, they were unable to significantly stimulate the invasion capacity of cells grown under these conditions (Fig. 3f). Nevertheless, fibroblasts activated matrix metalloproteases (MMPs) in both MTT control and *Sdhb*-silenced cells in the presence of Matrigel (Fig. 3g). Basal MMP activity in single culture was significantly lower in *Sdhb*-silenced cells compared to control, resulting also in a lower absolute MMP activity for *Sdhb*-silenced cells when conditioned by fibroblasts. The relative increase of MMP activity with fibroblast was, however, much greater in the *Sdhb* knockdown compared to control (4.8-fold versus 2.1-fold).

In addition to growth and pro-metastatic features, we evaluated fibroblast-mediated effects on cell metabolism. Measurements of intracellular ATP in co-cultured MTT cells showed a significant decrease only in Sdhb63 cells, indicating that fibroblasts stimulate the use of intracellular ATP, which the TCA-impaired cells cannot fully compensate for (Fig. 4a). These results are supported by intracellular measurements of Krebs cycle metabolites and amino acids, showing an additional decrease of citrate, *cis*-aconitate, isocitrate, aspartate and glutamate in fibroblast-co-cultured *Sdhb*-silenced MTT cells compared to single culture (Fig. 4b, c).

Sdhb-silenced MTT cells significantly increased glucose uptake by 70% compared to control and lactate uptake by twofold, resulting in a comparable increase in intracellular lactate levels without any changes to extracellular lactate concentrations (Fig. 5a–d). These features were even more prominent when silenced cells were co-cultured with primary fibroblasts, with glucose and lactate uptake being additionally increased by 60% and 104%, respectively, compared to single culture. Control MTT cells only showed an elevation in glucose uptake of 48%, with no change in lactate. These data suggest that lactate is an important metabolic substrate for *Sdhb*-silenced but not for *Sdhb* wild-type cells.

Fibroblasts under co-culture conditions did not show differences in either glucose or lactate uptake; however, they released significantly higher amounts of lactate into the culture medium (Fig. 5d). In line with this observation, co-culture-stimulated fibroblasts were also found to have significantly increased protein levels of monocarboxylate transporter 4 (MCT4), responsible for transporting lactate from the cytoplasm to the extracellular space (Fig. 5e, e'). Extracellular lactate alone has no stimulating effect on MTT cell proliferation (data not shown) but may provide carbons for anabolic metabolism.

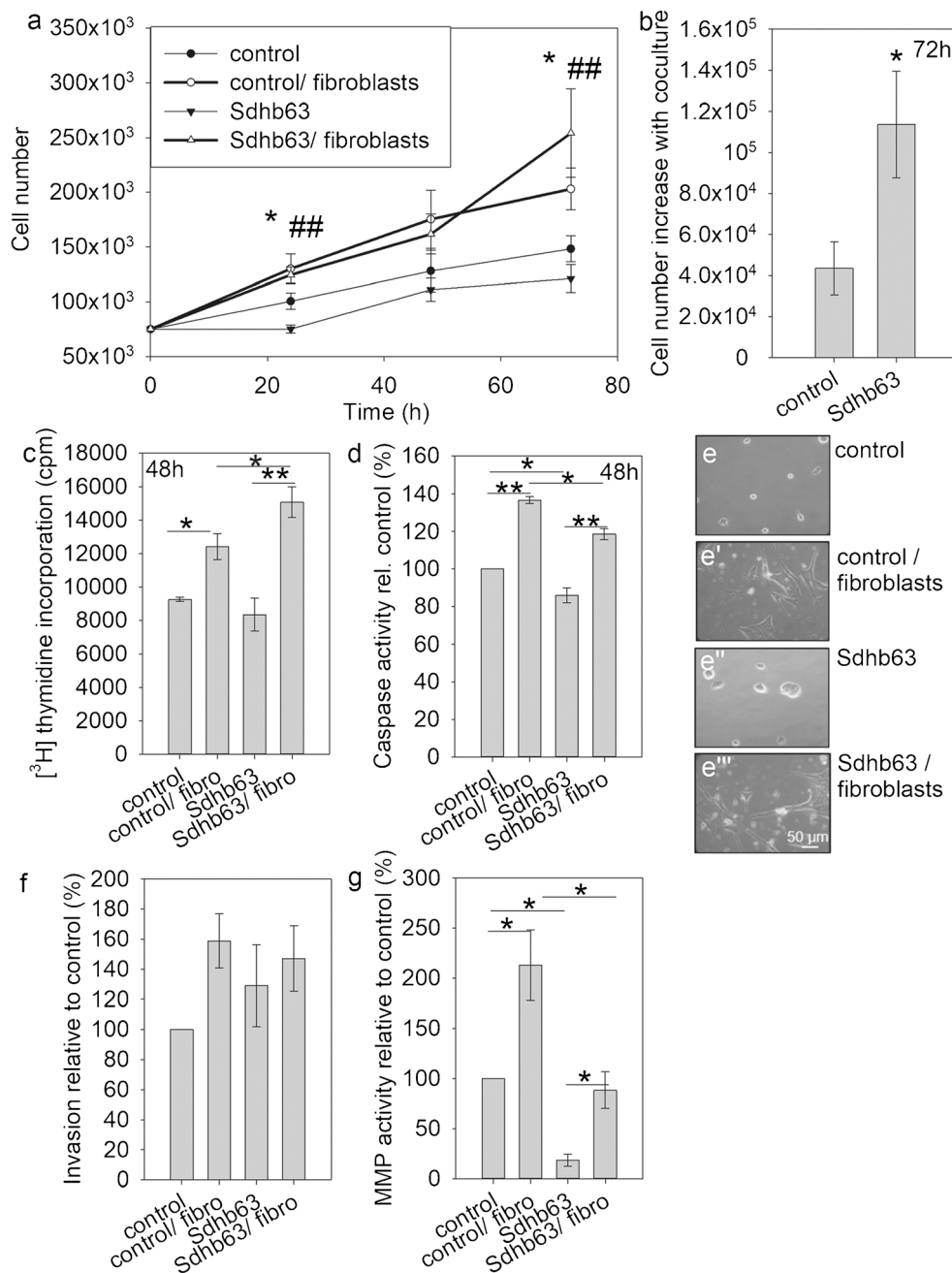
Discussion

This study shows that *Sdhb* knockdown-impaired cell growth can be reversed by co-culture with primary fibroblasts, addressing a paradox about how tumorigenesis can result from loss of succinate dehydrogenase function and associated TCA cycle impairment. In parallel, we also show that co-culture stimulates changes in energy pathway metabolism and invasive processes.

Loss of functional activity of succinate dehydrogenase affects cellular energy production by blocking the TCA cycle, thereby negatively impacting efficient production of reducing equivalents and the mitochondrial electron transport chain. It is therefore not unexpected that *Sdhb* knockdown leads to decreased proliferative capacity, as shown in the present study, when maximum amounts of nutrients and growth factors are available. This finding is also in agreement with other cell line studies where *Sdhb* knockdown or silencing also resulted in decreased proliferation (Cardaci et al. 2015; Cervera et al. 2008; Letouze et al. 2013). This feature represents a shortcoming of simple in vitro model systems that is particularly relevant to their use in therapeutic drug development.

Functional SDH impairment in our model was demonstrated by increased succinate-to-fumarate ratio, decreased respiratory capacity and intracellular Krebs cycle and amino acid concentrations. The nature of the incomplete *Sdhb* knockdown by shRNA of about 60% is apparent in the magnitude of the increase in succinate to fumarate. In human tumors,

Fig. 3 Fibroblast co-culture stimulates proliferation but not invasion in MTT control and *Sdhb* knockdown cells in monolayer. **a** Cell numbers were counted over a period of 72 h in serum-starved cultures alone or with fibroblast co-culture. Four independent experiments with duplicate cultures each are displayed. Asterisks (* control vs control/ fibroblasts, # *Sdhb63* versus *Sdhb63*/fibroblasts) indicate significance ($p < 0.05$, $p < 0.001$) by least square multivariate analysis with the Tukey-Kramer post hoc test. **b** Cell number increase with fibroblast co-culture relative to serum starvation after 72 h. Asterisks show significance by the Wilcoxon rank-sum test. **c** Thymidine incorporation measured in three experiments. **d** Caspase activity assessed in three experiments. **e**, **e'**, **e''**, **e'''** Photos were taken at $\times 10$ objective magnification after 72 h of culture. **f** Invasion measured by Transwell assay in three experiments. **g** Matrix metalloprotease activity measured in the presence of Matrigel, three experiments. Asterisks indicate significance ($*p < 0.05$) by one-way ANOVA with the Bonferroni post hoc test



elevations of 100-fold and more were determined and the *Sdhb* knockout in mouse chromaffin progenitor cells showed an increase of succinate of over 200-fold above control (Letouze et al. 2013; Richter et al. 2014). Again, that model like ours also showed delayed proliferation of *Sdhb*-silenced cells. Here, we additionally establish that reduction in SDHB protein does not lead to a significant change in clonogenic cell survival but does cause a significant increase in reductive capacity of MTT cells measured by reduction of tetrazolium salt. The latter may be explained by changes in the redox state, including increased cytoplasmic production of reducing equivalents or higher levels of normoxic reactive oxygen

species (Guzy et al. 2008). siRNA-mediated knockdown of *Sdhb* in rat PC12 cells did not lead to changes in cell viability, possibly due to the transient nature of silencing (Saito et al. 2016). Despite lower doubling time, *Sdhb*-impaired MTT cells appear more viable with comparable clonogenic survival, indicating that these cells may have an advantage when the right proliferative triggers are present.

Our finding that MTT cells with *Sdhb* knockdown have increased dopamine production in in vitro culture with serum is in agreement with other studies involving transient *Sdhb* knockdown in PC12 cells, where TH activity was induced through changes in serine phosphorylation (Daubner et al.

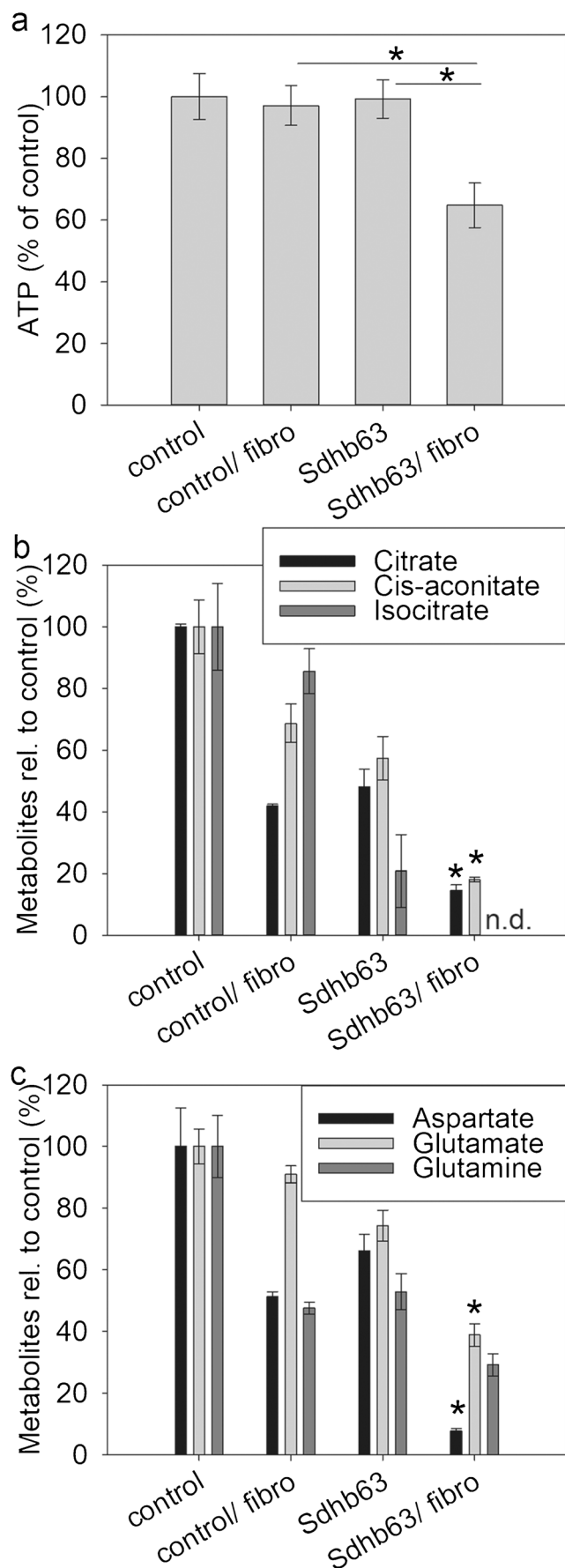


Fig. 4 Fibroblast co-culture additionally lowers energy reserves and central carbon metabolites in *Sdhb*-silenced MTT cells compared to control. **a** Intracellular ATP levels were measured in four independent experiments with two replicates each. **b, c** LC-MS/MS-mediated measurements in MTT cells with fibroblast co-culture of intracellular metabolites of selected Krebs cycle acids (**b**) and amino acids (**c**). Asterisks indicate significance by one-way ANOVA/Bonferroni test ($*p < 0.05$), comparing *Sdhb63* with and without co-culture; *n.d.* not detectable

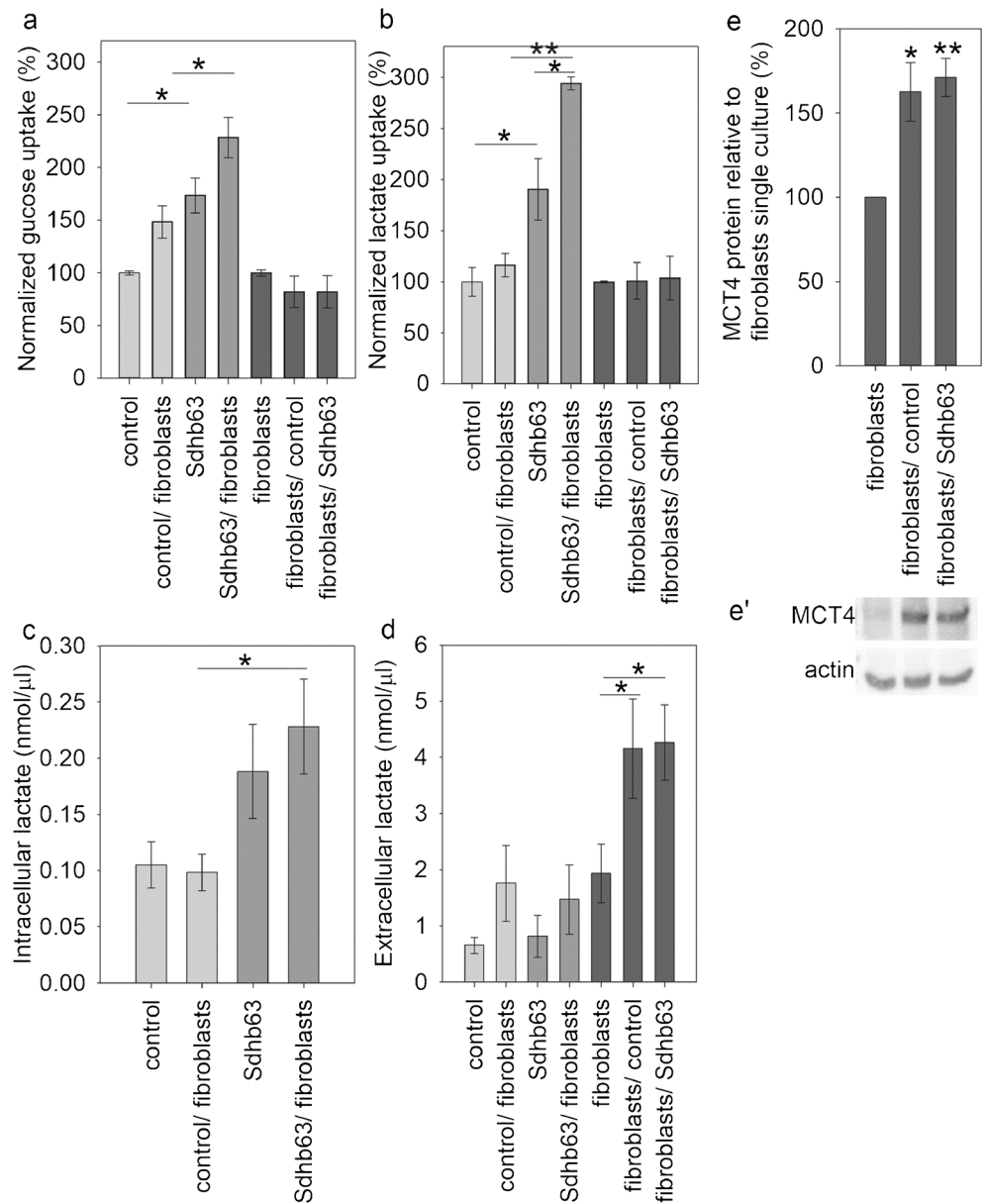
2011; Saito et al. 2016). Expression levels of genes encoding enzymes of the catecholamine synthesis pathway were unchanged with *Sdhb* knockdown, as previously shown in the human chromaffin progenitor cell line Pheo1 (Ghayee et al. 2013). This phenotype again does not recapitulate the clinical situation where catecholamine contents of *SDHB*-mutated tumors are markedly lower than those for other PHEOs/PGLs (4). Culture in serum-free medium, however, did not lead to catecholamine increase in *Sdhb*-silenced cells, suggesting a specific serum-dependent effect that may not occur in chromaffin cells in the human body.

Although *Sdhb*-impaired MTT cells appear more viable, our findings together with those of others that *Sdhb*-impaired cells exhibit reduced proliferative capacity are difficult to reconcile against the uncontrolled growth associated with PHEOs/PGLs that arise due to mutations of *SDHB*. This is particularly relevant when it is considered that such tumors are much more aggressive and prone to malignancy than those due to other mutations. These inconsistencies in experimental and clinical observations are now reconciled here by findings that co-culture with fibroblasts resulted in the reversal of the impaired cellular proliferation of *Sdhb*-impaired MTT cells. Specifically, we show that proliferation of MTT cells is stimulated by co-culture with primary fibroblasts and that the growth delay of *Sdhb*-impaired compared to wild-type cells was reversed under these conditions. These findings implicate the tumor microenvironment in influencing tumor cell proliferation, clarifying why *Sdhb*-impaired cells in monoculture do not recapitulate the clinical situation. Here, we would like to emphasize that CAFs were only able to induce proliferation in the absence of serum, since high proliferative rates associated with serum culture masked fibroblast-driven effects.

In the future, it will be interesting to investigate whether a similar phenotypic switch occurs when these MTT cells are grafted on mice. Other studies using mouse or rat PHEO models have shown that such in vivo models correlate with the clinical presentation of PHEO/PGL (Ullrich et al. 2014; Wiedemann et al. 2016).

CAFs are known to release a wide variety of survival and growth factors and induce metabolic changes in a number of different tumor cells (Chiarugi and Cirri 2016; Hanahan and Coussens 2012; Quail and Joyce 2013). To date, this effect has not been shown in monolayer culture for chromaffin cells, only in developmentally related neuroblastoma cells (Rapizzi et al. 2015).

Fig. 5 Fibroblast co-culture stimulates metabolism of *Sdhb* knockdown MTT cells by secreting lactate into the extracellular space. Glucose (a) and lactate (b) uptake as well as intracellular (c) and extracellular (d) lactate were measured in three experiments with two replicates each. e Densitometry of western blot results for MCT4 in fibroblasts with and without co-culture; $n = 4$. e' Representative blot displayed under the graph. Asterisks indicate significance ($*p < 0.05$, $**p < 0.01$) by one-way ANOVA with the Bonferroni post hoc test or Dunnett's post hoc test



Interestingly, intracellular ATP and metabolites of the central carbon metabolism were decreased in co-cultured *Sdhb* knockdown cells, suggesting a mobilization of ATP and metabolic resources towards energy-consuming processes, such as proliferation and invasiveness. Although monolayer culture did not show clear effects towards increased invasion, the use of a three-dimensional culture model of the same cell lines demonstrated a strong fibroblast-mediated increase in cellular outgrowth from spheroids embedded in Matrigel (D'Antongiovanni et al. 2017). Under these conditions, we established a phenotype of collective cell migration for *Sdhb*-silenced but not control MTT cells. In monolayer culture, we observed a trend towards decreased adhesive capacity. This phenotype might have obscured small increases in cell migration and invasion due to the applied method, where only cells attached to the lower surface of the membrane were quantified.

Previous work demonstrated that CAFs are reprogrammed to a glycolytic Warburg phenotype upon contact with tumor cells leading to enhanced lactate secretion (Chiarugi and Cirri 2016; Fiaschi et al. 2012; Rapizzi et al. 2015). The latter effect was shown for primary fibroblasts after co-culture with MTT cells, although glucose uptake was found to be unchanged. Lactate secreted by fibroblasts via MCT4 was preferentially used by *Sdhb*-silenced cells. Co-culture strongly increased lactate and also glucose uptake in these cells over the already elevated basal levels. Control MTT cells, on the contrary, did not change lactate uptake with co-culture but showed some increase in glucose uptake. These results demonstrate elevated susceptibility of *Sdhb* knockdown MTT cells to lactate, which will be most likely used for anabolic processes, such as replenishing aspartate pools, as has been shown for pyruvate

in *Sdhb* knockout cell lines (Cardaci et al. 2015; Lussey-Lepoutre et al. 2015). Interestingly, in contrast to these previously published models, *Sdhb* knockdown in MTT cells does not lead to an increase in lactate secretion. This difference might be due to the genetic background of MTT cells, originating from mouse PHEOs in heterozygous-deficient neurofibromin 1 mice with further genetic aberrations after reinjection into mice (Martiniova et al. 2009; Masgras et al. 2017).

Unraveling the biological basis of tumorigenesis in *SDHB*-mutated PGLs and improving model systems are essential for developing new pharmacological approaches for treatment of metastatic PHEO/PGL. Targeting the cross-talk between tumor cells and the microenvironment provides another avenue besides tumor cell-directed approaches for therapy.

Acknowledgements We thank Dr. Arthur Tischler and Dr. Lucia Martiniova, who generated mouse pheochromocytoma cells (MPCs) and mouse tumor tissue (MTT)-derived cells, respectively.

Funding information This work was supported by the Paradifference Foundation, the Fondazione Cassa di Risparmio di Pistoia e Pescia (Prot. 2016.0241/gi; to M.M.) and the Deutsche Forschungsgemeinschaft (RI 2684/1-1; CRC/TRR 205—project B10 to S.R. and project B12 to G.E.). This research was supported, in part, by the Intramural Research Program of the NIH, NICHD.

Compliance with ethical standards

Conflict of interest The authors declare that they have no conflicts of interest.

References

- Aspuria PJ, Lunt SY, Varembo L, Vergnes L, Gozo M, Beach JA, Salumbides B, Reue K, Wiedemeyer WR, Nielsen J, Karlan BY, Orsulic S (2014) Succinate dehydrogenase inhibition leads to epithelial-mesenchymal transition and reprogrammed carbon metabolism. *Cancer Metab* 2:21
- Cardaci S, Zheng L, MacKay G, van den Broek NJ, MacKenzie ED, Nixon C, Stevenson D, Tumanov S, Bulusu V, Kamphorst JJ, Vazquez A, Fleming S, Schiavi F, Kalna G, Blyth K, Strathdee D, Gottlieb E (2015) Pyruvate carboxylation enables growth of SDH-deficient cells by supporting aspartate biosynthesis. *Nat Cell Biol* 17:1317–1326
- Cervera AM, Apostolova N, Crespo FL, Mata M, McCreath KJ (2008) Cells silenced for SDHB expression display characteristic features of the tumor phenotype. *Cancer Res* 68:4058–4067
- Chiarugi P, Cirri P (2016) Metabolic exchanges within tumor microenvironment. *Cancer Lett* 380:272–280
- D'Antongiovanni V, Martinelli S, Richter S, Canu L, Guasti D, Mello T, Romagnoli P, Pacak K, Eisenhofer G, Mannelli M, Rapizzi E (2017) The microenvironment induces collective migration in SDHB-silenced mouse pheochromocytoma spheroids. *Endocr Relat Cancer* 24:555–564
- Daubner SC, Le T, Wang S (2011) Tyrosine hydroxylase and regulation of dopamine synthesis. *Arch Biochem Biophys* 508:1–12
- Eisenhofer G, Goldstein DS, Stull R, Keiser HR, Sunderland T, Murphy DL, Kopin IJ (1986) Simultaneous liquid-chromatographic determination of 3,4-dihydroxyphenylglycol, catecholamines, and 3,4-dihydroxyphenylalanine in plasma, and their responses to inhibition of monoamine oxidase. *Clin Chem* 32:2030–2033
- Eisenhofer G, Lenders JW, Siegert G, Bornstein SR, Friberg P, Milosevic D, Mannelli M, Linehan WM, Adams K, Timmers HJ, Pacak K (2012) Plasma methoxytyramine: a novel biomarker of metastatic pheochromocytoma and paraganglioma in relation to established risk factors of tumour size, location and SDHB mutation status. *Eur J Cancer* 48:1739–1749
- Favier J, Amar L, Gimenez-Roqueplo AP (2015) Paraganglioma and pheochromocytoma: from genetics to personalized medicine. *Nat Rev Endocrinol* 11:101–111
- Fiaschi T, Marini A, Giannoni E, Taddei ML, Gandellini P, De Donatis A, Lanciotti M, Serni S, Cirri P, Chiarugi P (2012) Reciprocal metabolic reprogramming through lactate shuttle coordinately influences tumor-stroma interplay. *Cancer Res* 72:5130–5140
- Ghayee HK, Bhagwandin VJ, Stastny V, Click A, Ding LH, Mizrahi D, Zou YS, Chari R, Lam WL, Bachoo RM, Smith AL, Story MD, Sidhu S, Robinson BG, Nwariaku FE, Gazdar AF, Auchus RJ, Shay JW (2013) Progenitor cell line (hPheo1) derived from a human pheochromocytoma tumor. *PLoS One* 8:e65624
- Gimenez-Roqueplo AP, Favier J, Rustin P, Rieubland C, Crespin M, Nau V, Khau Van Kien P, Corvol P, Plouin PF, Jeunemaitre X (2003) Mutations in the SDHB gene are associated with extra-adrenal and/or malignant pheochromocytomas. *Cancer Res* 63:5615–5621
- Guzy RD, Sharma B, Bell E, Chandel NS, Schumacker PT (2008) Loss of the SdhB, but not the SdhA, subunit of complex II triggers reactive oxygen species-dependent hypoxia-inducible factor activation and tumorigenesis. *Mol Cell Biol* 28:718–731
- Hanahan D, Coussens LM (2012) Accessories to the crime: functions of cells recruited to the tumor microenvironment. *Cancer Cell* 21:309–322
- Imperiale A, Moussallieh FM, Sebag F, Brunaud L, Barlier A, Elbayed K, Bachellier P, Goichot B, Pacak K, Namer IJ, Taieb D (2013) A new specific succinate-glutamate metabolomic hallmark in sdhx-related paragangliomas. *PLoS One* 8:e80539
- Jochmanova I, Pacak K (2016) Pheochromocytoma: the first metabolic endocrine cancer. *Clin Cancer Res: Off J Am Assoc Cancer Res* 22:5001–5011
- King KS, Prodanov T, Kantorovich V, Fojo T, Hewitt JK, Zacharin M, Wesley R, Lodish M, Raygada M, Gimenez-Roqueplo AP, McCormack S, Eisenhofer G, Milosevic D, Kebebew E, Stratakis CA, Pacak K (2011) Metastatic pheochromocytoma/paraganglioma related to primary tumor development in childhood or adolescence: significant link to SDHB mutations. *J Clin Oncol Off J Am Soc Clin Oncol* 29:4137–4142
- Letouze E, Martinelli C, Lorient C, Burmichon N, Abermil N, Ottolenghi C, Janin M, Menara M, Nguyen AT, Benit P, Buffet A, Marcaillou C, Bertherat J, Amar L, Rustin P, De Reynies A, Gimenez-Roqueplo AP, Favier J (2013) SDH mutations establish a hypermethylator phenotype in paraganglioma. *Cancer Cell* 23:739–752
- Lussey-Lepoutre C, Hollinshead KE, Ludwig C, Menara M, Morin A, Castro-Vega LJ, Parker SJ, Janin M, Martinelli C, Ottolenghi C, Metallo C, Gimenez-Roqueplo AP, Favier J, Tennant DA (2015) Loss of succinate dehydrogenase activity results in dependency on pyruvate carboxylation for cellular anabolism. *Nat Commun* 6:8784
- Mannelli M, Rapizzi E, Fucci R, Canu L, Ercolino T, Luconi M, Young WF Jr (2015) 15 years of paraganglioma: metabolism and pheochromocytoma/paraganglioma. *Endocr Relat Cancer* 22:T83–T90
- Martiniova L, Lai EW, Elkahloun AG, Abu-Asab M, Wickremasinghe A, Solis DC, Perera SM, Huynh TT, Lubensky IA, Tischler AS, Kvetnansky R, Alesci S, Morris JC, Pacak K (2009) Characterization of an animal model of aggressive metastatic pheochromocytoma linked to a specific gene signature. *Clin Exp Metastasis* 26:239–250
- Masgras I, Ciscato F, Brunati AM, Tibaldi E, Indraccolo S, Curtarello M, Chiara F, Cannino G, Papaleo E, Lambrughi M, Guzzo G, Gambalunga A, Pizzi M, Guzzardo V, Rugge M, Vuljan SE,

- Calabrese F, Bernardi P, Rasola A (2017) Absence of neurofibromin induces an oncogenic metabolic switch via mitochondrial ERK-mediated phosphorylation of the chaperone TRAP1. *Cell Rep* 18:659–672
- Pamporaki C, Hamplova B, Peitzsch M, Prejbisz A, Beuschlein F, Timmers HJ, Fassnacht M, Klink B, Lodish M, Stratakis CA, Huebner A, Fliedner S, Robledo M, Sinnott RO, Januszewicz A, Pacak K, Eisenhofer G (2017) Characteristics of pediatric vs adult pheochromocytomas and paragangliomas. *J Clin Endocrinol Metab*
- Quail DF, Joyce JA (2013) Microenvironmental regulation of tumor progression and metastasis. *Nat Med* 19:1423–1437
- Rapizzi E, Ercolino T, Fucci R, Zampetti B, Felici R, Guasti D, Morandi A, Giannoni E, Giache V, Bani D, Chiarugi A, Mannelli M (2014) Succinate dehydrogenase subunit B mutations modify human neuroblastoma cell metabolism and proliferation. *Hormones Cancer* 5:174–184
- Rapizzi E, Fucci R, Giannoni E, Canu L, Richter S, Cirri P, Mannelli M (2015) Role of microenvironment on neuroblastoma SK-N-AS SDHB-silenced cell metabolism and function. *Endocr Relat Cancer* 22:409–417
- Richter S, Peitzsch M, Rapizzi E, Lenders JW, Qin N, de Cubas AA, Schiavi F, Rao JU, Beuschlein F, Quinkler M, Timmers HJ, Opocher G, Mannelli M, Pacak K, Robledo M, Eisenhofer G (2014) Krebs cycle metabolite profiling for identification and stratification of pheochromocytomas/paragangliomas due to succinate dehydrogenase deficiency. *J Clin Endocrinol Metab* 99:3903–3911
- Saito Y, Ishii KA, Aita Y, Ikeda T, Kawakami Y, Shimano H, Hara H, Takekoshi K (2016) Loss of SDHB elevates catecholamine synthesis and secretion depending on ROS production and HIF stabilization. *Neurochem Res* 41:696–706
- Ullrich M, Bergmann R, Peitzsch M, Cartellieri M, Qin N, Ehrhart-Bornstein M, Block NL, Schally AV, Pietzsch J, Eisenhofer G, Bornstein SR, Ziegler CG (2014) In vivo fluorescence imaging and urinary monoamines as surrogate biomarkers of disease progression in a mouse model of pheochromocytoma. *Endocrinology* 155:4149–4156
- Wiedemann T, Peitzsch M, Qin N, Neff F, Ehrhart-Bornstein M, Eisenhofer G, Pellegata NS (2016) Morphology, biochemistry, and pathophysiology of MENX-related pheochromocytoma recapitulate the clinical features. *Endocrinology* 157:3157–3166